Improved GSO Algorithms and Their Applications in Multi-Target Detection and Tracking Field

XINGKUI XU[ID][1], QINGYU HOU[1], CHUNFENG WU[1,2], AND ZHIGANG FAN[1]
[1]Research Center for Space Optical Engineering, Harbin Institute of Technology, Harbin 150001, China
[2]China Space Sanjiang Group Corporation Ltd., Wuhan 430040, China

Corresponding author: Qingyu Hou (houqingyu@126.com)

ABSTRACT Fast detection and high-precision tracking of multiple UAVs are the keys to achieving efficient low-altitude defense. However, as there are many hyper-parameters which need to be optimized in target detection network, commonly used methods such as random search method are computationally intensive and cannot quickly obtain multiple optimal hyper-parameters combinations. In addition, angular random walk due to low-frequency noise of speed sensor in servo loop can cause target tracking accuracy to decrease. Fortunately, those two problems can be regarded as a single-mode function optimization problem and a multi-mode function optimization problem, respectively. In the paper, in order to overcome the aforementioned problems, GSOM (glowworm swarm optimization mutation) algorithm and GSOMLDW (glowworm swarm optimization mutation linearly decreasing weight) algorithm are firstly proposed. Furthermore, the global convergence of GSOMLDW has been proven in the paper, which has not been analyzed in currently available literature. Then, experimental results on four multi-modal benchmark functions have strongly illustrated that the novel GSOM algorithm can enhance glowworms' memory ability and improve peak detection rate effectively. When it is used for optimizing hyper-parameters of multi-target detection network, it can be expected to obtain much more hyper-parameter combination selections. Meanwhile, experimental results on ten uni-modal benchmark functions have obviously demonstrated that GSOMLDW algorithm can balance glowworms' exploration and exploitation abilities powerfully and obtain superior global solution accuracy at last. When the GSOMLDW algorithm is used for servo system identification and drift error model identification, the final position error fluctuation after compensation is almost zero while it reaches 1500 *urad* before compensation. Consequently, the proposed method can effectively improve target tracking precision.

INDEX TERMS GSO, system identification, multi-modal functions, multi-target tracking, anti-UAVs.

I. INTRODUCTION

With the popularization of UAVs (unmanned aerial vehicles, UAVs) in various fields, their characteristics that they can be equipped with functional equipments casually and are subject to subjective awareness make them to be a serious threat to public safety [1]. Different types of anti-UAV systems exist in various countries around the world. Among them, the laser defense system will be an important development direction of low-altitude defense in the future due to its fast speed, high accuracy, and high cost-effectiveness. It mainly consists of target image detection and target servo tracking [2], [3].

The associate editor coordinating the review of this manuscript and approving it for publication was Min Wang[ID].

However, there exist problems in both of the two parts. On one hand, current target detection algorithms are mostly based on neural networks, and hyper-parameters selection of neural network models has a great impact on the final target detection results. For example, a complex model may own good expressive ability to process different types of data. However, it may be impossible to be trained as gradient disappears due to too many layers. At present, methods such as grid search and random search methods are often used to select appropriate hyper-parameters. However, those algorithms have disadvantage of large amount of calculation. Thus, unreasonable selection of hyper-parameters may cause unsatisfactory detection results especially when the detection background is complex and there are multiple targets to

be detected. At present, grid search method and random search method are often used to obtain hyper-parameters for target detection network models. Unfortunately, these methods have certain disadvantages such as large calculation amount [4]. On the other hand, affected by non-linear drift error of gyro sensor, servo tracking accuracy is often not ideal. Usually, a low-frequency drift error model is established. Based on the error model and classical control methods, target servo tracking performance can be improved [5]–[7]. Fortunately, the above-mentioned two problems can be classified as a single-objective optimization problem and a multi-objective optimization problem, respectively. Therefore, they can be solved by popular swarm intelligence optimization algorithms.

In fact, swarm intelligence optimization algorithms have developed greatly and have been well applied in many fields [8]–[14] during recent years. For example, bee colony (BC) algorithm is motivated from bee colonies' nature behaviors. Genetic algorithm (GA) is inspired by natural selection and genetic mechanism [15]. Simulated annealing (SA) algorithm is based on solid annealing principles proposed by Kirkpatrick in 1983 [16]. Glowworm swarm optimization (GSO) algorithm is proposed through simulating nature glowworms' behavior [17]. Compared with traditional optimization methods, those swarm intelligence algorithms are more effective and have been utilized to solve complex non-linear optimization problems [13], [17]–[23].

Different from other swarm intelligence algorithms, GSO algorithm which is different from FA algorithm [24] owns both local optimum location ability and global optimum location ability. That means it is good at solving not only uni-modal optimization problems but also multi-modal optimization problems. Furthermore, it has many advantages such as powerful local search ability, several parameters to adjust, convenient operation and easy implementation [25].

All the things have made it very popular in many fields. For example, it has been effectively used in aspects of indoor localization [26], dispatching system of public transit vehicles [27], multi-modal functions for collective robotics applications [28], signal source localization for multi-robot system [29], node deployment strategy for WSNs [30], wiener system identification for three-dimensional elliptical vibration cutting [31], three-dimensional path planning for unmanned aerial vehicles [32], CWMN spectrum allocation [33] etc.

Unfortunately, when optimizing multi-mode functions the algorithm has its own shortcomings, such as premature convergence, low peak detection rate and poor convergence accuracy [34]. According to current literature, there are few studies about solving the problem. In this paper, in order to make up for the deficiency, mutation operation is first introduced into the original GSO algorithm to preserve its diversity and enhance its memory ability. Then, based on inertia weight technique [35] glowworm individual's movement step is adjusted to avoid premature convergence and improve optimization accuracy.

This paper is organized as follows. Firstly, section 2 describes composition of target detection and tracking system. Section 3 introduces the original GSO algorithm and the improved GSO algorithms which include GSOM algorithm and GSOMLDW algorithm. Multi-target detection framework based on GSOM algorithm and target servo tracking framework based on GSOMLDW algorithm are described in section 4. Then, analysis of simulation and experimental results is shown in section 5. Specifically, effectiveness verification of GSOM algorithm and its application in hyper-parameter training for multi-target detection network is shown in section 5.1. Section 5.2 provides effectiveness verification of GSOMLDW algorithm and its application in servo system identification and sensor drift error compensation. Finally, section 6 concludes the work in the paper.

II. COMPOSITION OF TARGET DETECTION AND TRACKING SYSTEM

As shown in Fig.1, the entire low-altitude defense system can be divided into three parts, i.e., a multi-target detection module based on image processing, a target servo tracking module equipped with a photoelectric turntable, and a mobile vehicle central control system. Among them, image processing based multi-target detection module is mainly composed of a visible light sensor and a GPS sensor. Internal measurement sensor, raster position sensor and motor drivers form the servo tracking module. Additionally, the vehicle-mounted central control system is mainly responsible for upper-layer decision-making processing, and it uses wireless communication equipment to exchange information with vehicle-mounted embedded systems. Furthermore, the vehicle-mounted embedded system contributes to designing the underlying algorithms, which comprises of vision module controller, rough ring U-frame controller, fast mirror controller, transmission system controller and drive system controller.

III. DESCRIPTION OF THE ORIGINAL GSO ALGORITHM, THE PROPOSED GSOM ALGORITHM AND GSOMLDW ALGORITHM
A. GLOWWORM SWARM OPTIMIZATION (GSO) ALGORITHM

In GSO algorithm [17], [18], each glowworm individual has its own perceptual radius which determines its search range. After many iterations, most of glowworms cluster at certain points. These points represent the locally or globally optimal solutions of the considered objective functions. The whole principle is composed of three phases and is described as follows:

1) FLUORESCEIN UPDATE PHASE
At the beginning, each glowworm's value of fluorescein is equal. However, the fluorescein volatilizes over time. In order to simulate the characteristic, at every iteration each glowworm's fluorescein value is changed according to the
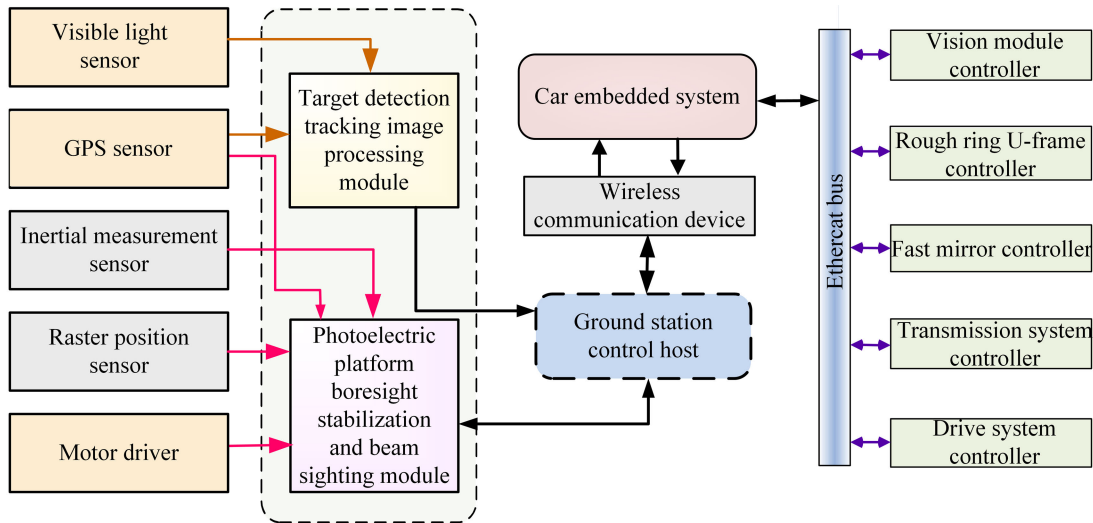
FIGURE 1. The composition of target detection and tracking system.

following equation.

$$g_i(t) = (1 - d)g_i(t - 1) + \alpha \times f(p_i(t)) \qquad (1)$$

In the above equation, $g_i(t)$ represents the ith glowworm's fluorescein level at the tth iteration, $p_i(t)$ is the ith glowworm's location and $f(p_i(t))$ is the objective function value of the ith glowworm at the tth iteration. Additionally, $d(0 < d < 1)$ and α represent decay constant and fluorescein enhancement constant, respectively.

2) MOVEMENT PHASE

Each individual i needs to select a better individual j within its sensor radius, and selection probabilistic is depicted as below:

$$G_{ij}(t) = \frac{g_j(t) - g_i(t)}{\sum_{k \in L_i(t)} g_k(t) - g_i(t)} \qquad (2)$$

where $g_i(t)$ represents the fluorescein value of the ith glowworm individual at the tth iteration. $g_j(t)$ represents the fluorescein value of the jth glowworm individual at the tth iteration. $L_i(t)$ represents a set of individuals with larger fluorescein value than glowworm individual i within its perceived radius at the tth iteration. K is the Kth glowworm individual in the L set.

The detail of $L_i(t)$ is shown in the following equation:

$$L_i(t) = \{j : \|p_j(t) - p_i(t)\| < r_d^i(t); g_i(t) < g_j(t)\} \qquad (3)$$

It behaves numbers of the ith glowworm's neighbors within its decision radius at the tth iteration. In the equation, $\|p_j(t) - p_i(t)\|$ is euclidian distance between glowworm i and glowworm j, and $r_d^i(t)$ is the ith glowworm's decision radius at the tth iteration. Additionally, $g_i(t)$ and $g_j(t)$ are the ith and the jth glowworm's fluorescein level at the tth iteration. According to Eq.(2), glowworm i will move to the next position:,

$$p_i(t + 1) = p_i(t) + s \times (\frac{p_j(t) - p_i(t)}{\|p_j(t) - p_i(t)\|}) \qquad (4)$$

where s is movement step.

3) LOCAL-DECISION RANGE UPDATE PHASE

Each glowworm i has its own dynamic decision domain:

$$r_d^i(t + 1) = min\{r_s, max\{0, r_d^i(t) + \beta(l_t - |L_i(t)|)\}\} \qquad (5)$$

In the above equation, $r_d^i(t)$ satisfies $0 < r_d^i < r_s$. r_s is its sensor radius, β is neighbor-domain's change rate and l_t is threshold of neighbor numbers.

B. GLOWWORM SWARM OPTIMIZATION MUTATION (GSOM) ALGORITHM

GSO algorithm has powerful local search ability and it is often utilized to solve multi-modal optimization problems. However, each individual's movement depends on better individuals' existence within its perception range. If there is no outstanding ones, the individual will move nowhere. Thus, it may lead to low convergence rate and low peak detection rate when dealing with multi-modal optimization problems. That means it may miss many other locally extreme points.

The part of work introduces mutation operation [17] into GSO algorithm. When a glowworm steps into a trap and there are no better individuals within its perception range, a new individual will be produced according to mutation operation as depicted below:

$$p_i(t + 1) = p_i(t) + s1 \times (\frac{Globalbest - p_i(t)}{\|Globalbest - p_i(t)\|})$$
$$+ s2 \times (\frac{Singlebest - p_i(t)}{\|Singlebest - p_i(t)\|}) \qquad (6)$$

where "Globalbest" behaves the best solution ever found by all the glowworms. "Singlebest" behaves the best solution ever found by the currently considered glowworm i. s1 and s2 are both movement steps.

Thus, when the new individual is better, it will replace the old one. From the above equation, it can be easily seen that the behavior can make full use of all the glowworms' search history to locate local and global solutions.

C. GLOWWORM SWARM OPTIMIZATION MUTATION LINEARLY DECREASING WEIGHT (GSOMLDW) ALGORITHM

During optimization process, each glowworm finds a better neighbor within its perception range and moves close to it with a fixed movement step. With increase of iteration number, the distances between individuals and peaks become smaller and smaller. If the fixed step is larger than distances between individuals and peaks, individuals will move to the other side of a peak. Thus, a shock phenomenon occurs and individuals fail to reach the optimal solutions eventually. Under extreme conditions, when fluorescent values of all the individuals are the same, the algorithm cannot converge to peaks much more likely.

Here, on the basis of GSOM algorithm, we introduces inertia weight factor into position update formulas of individuals to overcome the above-mentioned disadvantage. Inertia weight [35] is described in the following equation:

$$\omega(t) = \frac{t_{max} - t}{t_{max}}(\omega_{max} - \omega_{min}) + \omega_{min} \qquad (7)$$

where t behaves current iteration number and ω is inertia weight.

At the moment, each glowworm can update its position according to the following formula:

$$p_i(t + 1) = \omega(t) \times p_i(t) + s \times (\frac{p_j(t) - p_i(t)}{\|p_j(t) - p_i(t)\|}) \qquad (8)$$

where $\omega(t)$ changes according to Eq.(7).

With technique of linearly decreasing inertia weight, movement step is shortened as iteration increases, which is beneficial to fully balance exploitation ability and exploration ability of GSO algorithm. The adaptive and variable step size can improve the algorithm's convergence speed, enhance its robustness and improve its convergence precision.

In the following part we will provide a simple proof about the global convergency of the proposed GSOMLDW algorithm:

Case1: $g[p_i(t + 1)] \leq g[p_i(t)]$ is met, where g is the fitness function.

Case2: if $\forall D \in S$, there is $M(D) > 0$ and $\prod_{k=0}^{\infty}(1 - P_k(D)) = 0$, where $p_i(t + 1)$ and $p_i(t)$ are glowworm i's positions at the $(t + 1)$th and tth respectively, D is the search domain, $M(D)$ is Lebesgue measure of D, $P_k(D)$ is probability measure of the kth iterative solution.

Theorem: If both of the above two cases are met, $E[p_i]$ is guaranteed to converge to the position with the best fitness, where E represents the finally expected value.

Proof: For case one, as the reason that GSOM algorithm owns mutation operator, the new solution can replace the old solution only when it is better than the old one. That means case one must always be met.

According to the location update equation, the following equation can be easily deduced:

$$p_i(t + 1) = w(t) \times p_i(t) + s \times \frac{p_j(t) - p_i(t)}{L} \qquad (9)$$

where $L = \|p_j(t) - p_i(t)\|$.

Let $\frac{S}{L} = \phi$, accordingly,

$$p_i(t + 1) = [w(t) - \phi] \times p_i(t) + \phi \times p_j(t) \qquad (10)$$

Thus,

$$E[p_i(t + 1)] - [w(t) - \phi] \times [p_i(t)] = \vartheta \qquad (11)$$

where $\vartheta = \phi \times p_j(t)$.

If position expectation of each glowworm is calculated, the following equation can be easily obtained:

$$m^2 - [w(t) - \phi] \times m + \xi = 0 \qquad (12)$$

where $m = E[p_i(t + 1)]$.

Therefore, the glowworms' position convergence problem can be transformed into an second-order equation problem. As long as $|\frac{w(t)-\phi\pm\sqrt{(w(t)-\phi)^2-4\vartheta}}{2}| < 1$ is satisfied, position trajectories of glowworms can be expected to converge to an optimal location finally.

Let ζ_i^t is the solution support set when glowworm i searches at the tth iteration. Therefore, when a better solution cannot be produced, the algorithm generates a random solution with the proposed method. That will make $\zeta_i^t = P$ real and lead to $\bigcup_{i=1}^{N} \zeta_i^t \supseteq P$ finally. For further analysis, $\forall D \in S, 0 < \sum_{i=1}^{N} p_k(D) \leq 1$ and $\prod_{k=0}^{\infty}(1 - p_k(D)) \longrightarrow lim_{k \longrightarrow \infty}(1 - 0 < \sum_{i=1}^{N} p_k(D) \leq 1)^k = 0$ can be deduced. At this time, case 2 is met. The conclusion that glowworms will finally converge to the optimal position has been proofed so far.

IV. MULTI-TARGET DETECTION AND TRACKING FRAMEWORK BASED ON GSOM AND GSOMLDW ALGORITHMS

On one hand, when the infrared sensor detects multiple targets in space, the targets' characteristic information can be obtained through signal processing and related algorithms. In order to identify targets in real time and reduce the false alarm rate, it is necessary to collect targets' off-line feature information, establish a target detection network and train the network based on the proposed GSOM algorithm. Specifically, after initializing GSOM's parameters, establishing fitness function, updating individuals' fluorescein and performing mutation operation, the deep network model is trained and the best model is obtained.

On the other hand, as high-frequency noise is mostly white noise, it is easier to remove. However, the low-frequency noise involved in the speed signal is random and uneven, and its energy is mainly concentrated in the low-frequency band. Therefore, conventional band-pass filters perform poorly and a low-frequency drift error compensation model needs to be established. In this paper the proposed GSOMLDW algorithm is used to identify the model's parameters. As Fig.2 shows, firstly it is necessary to perform frequency sweep processing on the photoelectric turntable to obtain parameters of the servo model. Then, gyroscope's data in different states is collected and preliminary low-pass filtering is performed. After that, GSOMLDW algorithm is
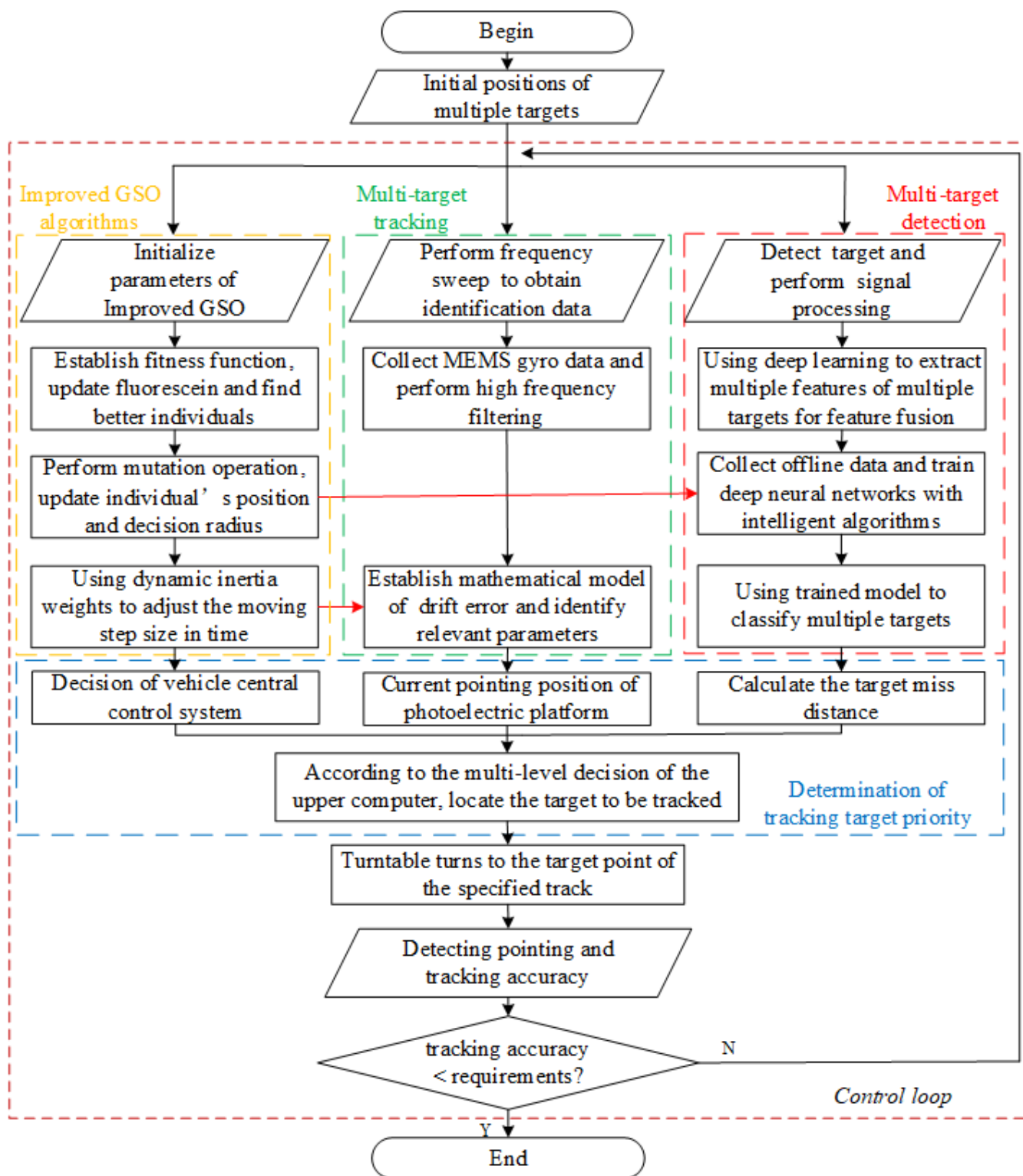
FIGURE 2. The framework for multi-target detection and tracking based on GSOM and GSOMLDW algorithms.

performed, during which dynamic inertia weight is used to adjust the moving step size in time so as to achieving a high-precision identification model for gyro error compensation. Finally, the steady-state error of the speed loop can be obtained and the target tracking accuracy can be expected.

At last, according to the upper-layer decision-making strategy, the target tracking priority is determined. Immediately,

off-target amount of the selected target is converted into the azimuth error and elevation error. Then, the turntable is controlled to continuously point and track the target until the target detection accuracy meets the requirements.

V. ANALYSIS OF SIMULATION AND EXPERIMENTAL RESULTS

A. EFFECTIVENESS VERIFICATION OF GSOM ALGORITHM AND ITS APPLICATION IN MULTI-TARGET DETECTION

1) EFFECTIVENESS VERIFICATION OF GSOM ALGORITHM

In order to test GSOM algorithm's multi-polar location ability, this section utilizes four multi-modal benchmark functions. Those functions have been shown in table 1.

TABLE 1. Multi-modal benchmark functions.

$$ff_1 = 200 - (x_1^2 + x_2 - 11)^2 - (x_1 + x_2^2 - 7)^2$$
$$ff_2 = -4 \times [(4 - 2.1 \times x_1^2 + \tfrac{x_1^4}{3}) \times x_1^2 + x_1 x_2 + (-4 + 4 \times x_2^2)]$$
$$ff_3 = -[\cos(2x_1 + 1) + 2\cos(3x_1 + 2) + 3\cos(4x_1 + 3)$$
$$+ 4\cos(5x_1 + 4) + 5\cos(6x_1 + 5)][\cos(2x_2 + 1)$$
$$+ 2\cos(3x_2 + 2) + 3\cos(4x_2 + 3) + 4\cos(5x_2 + 4) + 5\cos(6x_2 + 5)]$$
$$ff_4 = 0.5[\sin(10 \log x_1) + \sin(10 \log x_2)]$$

As depicted in literature [36], ff_1 contains four optimums which are located at (3.0, 2.0), (−3.87, −3.28), (3.58, −1.85) and (−2.81, 3.13), respectively. ff_2 which is ever used as a benchmark function in literature [9], [10] owns four optimums totally. ff_3 owns 778 unequal maxima [37]. ff_4 has 36 unevenly spaced but similar optimums. For more details regarding to those functions, please refer to literature [37].

When optimizing the above-mentioned functions, swarm population is set to be 500. For different functions, search domain, perception radius r_s and decision radius r_o are different. When the maximal iteration number is set to be 70, optimization results for ff_1, ff_2, ff_3 and ff_4 are presented in Fig.3 and Fig.4, respectively. a and b in Fig.3 exhibit glowworms' position distribution for function ff_1 with GSO algorithm and GSOM algorithm. c and d in Fig.4 exhibit glowworms' position distribution for function ff_2 with GSO algorithm and GSOM algorithm. a and b in Fig.3 exhibit glowworms' position distribution for function ff_3 with GSO algorithm and GSOM algorithm. c and d in Fig.4 exhibit glowworms' position distribution for function ff_4 with GSO algorithm and GSOM algorithm. Additionally, each red star represents one glowworm's position.

Optimization results illustrate that both GSOM and GSO algorithm can locate the four optimal points of function ff_1. However, optimization results for the other three multi-modal functions fully illustrate that the improved GSOM algorithm is more superior than the original GSO algorithm in solving multi-modal problems.

2) GSOM ALGORITHM FOR MULTI-TARGET DETECTION NETWORK TRAINING

For detection of multiple UAV targets in the air, the current method is to achieve the best combination of hyperparameters for the detection network model. This makes
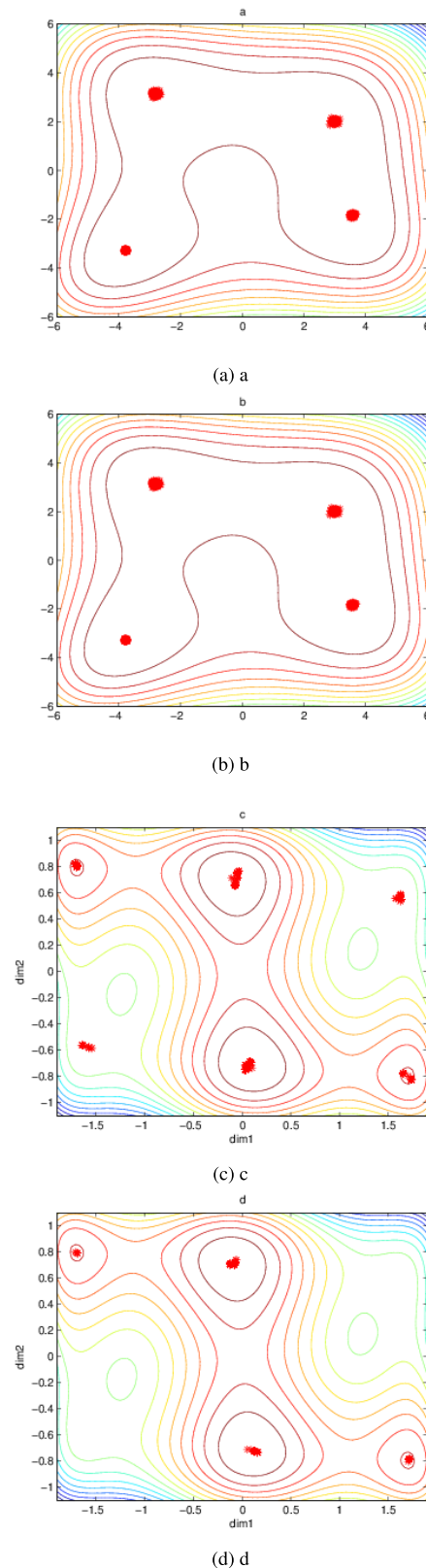

(a) a

(b) b

(c) c

(d) d

FIGURE 3. Glowworms' positions distribution for ff_1 and ff_2.

the network detect multiple UAV targets quickly and completely, facilitating subsequent targeting and tracking. Essentially it is a multi-mode function optimization problem.
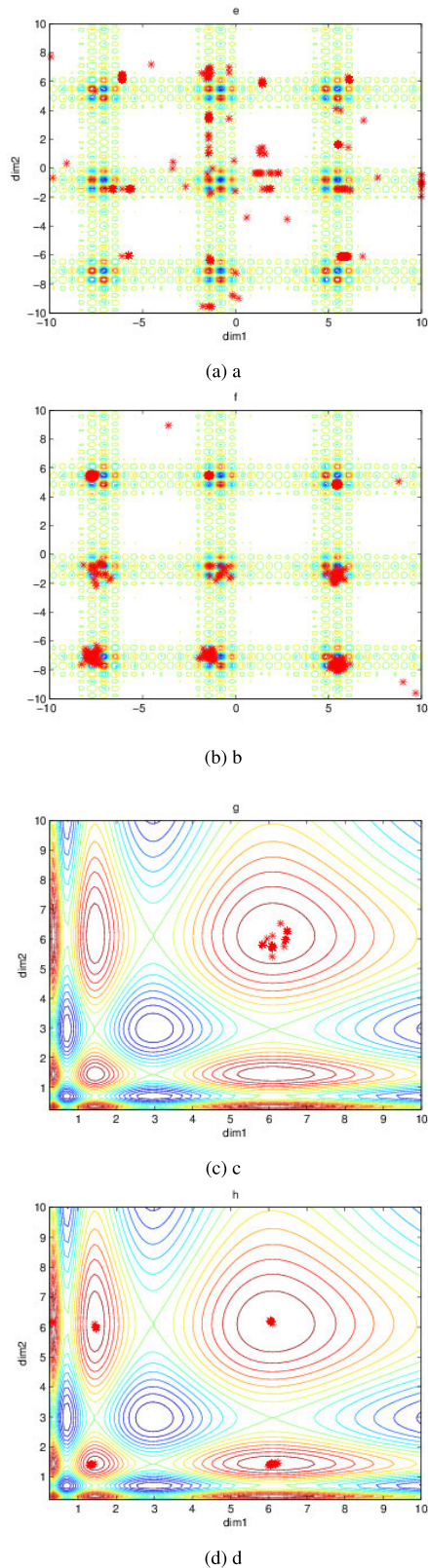
(a) a

(b) b

(c) c

(d) d

FIGURE 4. Glowworms' positions distribution for *ff*₃ and *ff*₄.

In order to simply and intuitively illustrate the superiority of the GSOM algorithm in solving multi-target detection problems, a complex multi-mode function is used here instead

of the detection network. The function is shown in Eq.(13). There are 25 maxima in the function and among them only one is the global maxima.

$$f = 500 - \frac{1}{0.002 + \sum_{i=0}^{24} \frac{1}{1+i+(x_1-a(i))^6+(x_2-b(i))^6}},$$
$$a(i) = 16 \times ((i \bmod 5) - 2), b(i) = 16 \times (\lfloor (i/5) \rfloor - 2) \quad (13)$$

Optimization results of GSOM algorithm and GSO algorithm at different iterations have been shown in Fig.5 and Fig.6. In Fig.5, a, b, c and d exhibit glowworms' position distribution at iteration 1, 90, 100 and 200 with GSOM algorithm, respectively. In the Fig.6, a, b, c and d exhibit glowworms' position distribution at iteration 1, 90, 100 and 200 with GSO algorithm, respectively. As can be seen from Fig.5, there are 25 optimal positions found finally by GSOM algorithm while the original GSO algorithm only finds 6 optimal points.

From above discussion, we can deduce that the improved GSOM algorithm is superior in solving multi-modal optimization problems and it strongly indicates that GSOM algorithm has a better application prospect in the field of multi-target detection. Specifically, with the proposed GSOMLDW algorithm many excellent hyper-parameter combinations for multi-target detection network can be obtained. That means an optimal model can be selected as the final network detection model among the obtained models according to our preference for other indicators such as calculation time cost, target detection accuracy, target detection position accuracy, model sensitivity to detection background, and model sensitivity to light interference. For example, among a bunch of effective models with low calculation time cost, a model with a higher accuracy rate may be selected as the final target detection network model for detecting multi-UAVs. Therefore, compared with GSO algorithm, better multi-UAVs detection results can be obtained with help of the proposed GSOM algorithm.

B. EFFECTIVENESS VERIFICATION OF GSOMLDW ALGORITHM AND ITS APPLICATION IN TARGET TRACKING SERVO SYSTEM

1) EFFECTIVENESS VERIFICATION OF GSOMLDW ALGORITHM

Ten functions have been given in table 2 to test GSOMLDW algorithm's performance.

Meanwhile, search domain and minimum value corresponding to each function have also been listed in the same table. Among the ten functions, several functions have a number of different locally optimal points such as f8. The locally optimal points constitute masses of traps. Under the circumstance, it is usually difficult for the primitive GSO algorithm to avoid premature and achieve a globally optimal value. Experimental results have been compared among GSO, LWGSO algorithm [38] and LWGSODE algorithm [38]. For more detailed information about LWGSO (linearly weight glowworm swarm optimization) algorithm
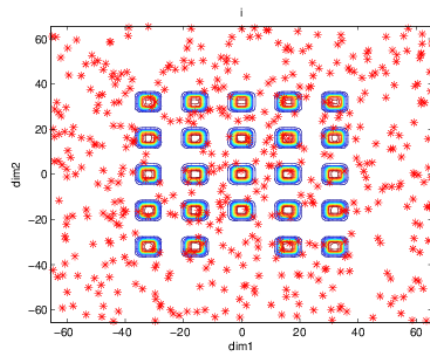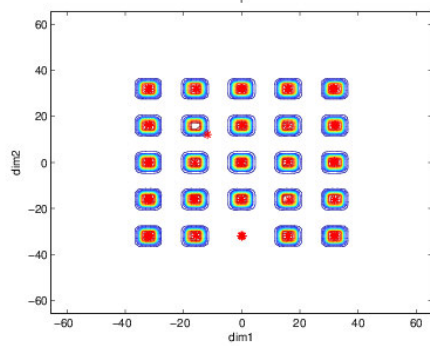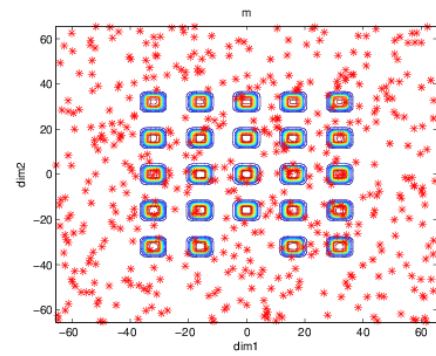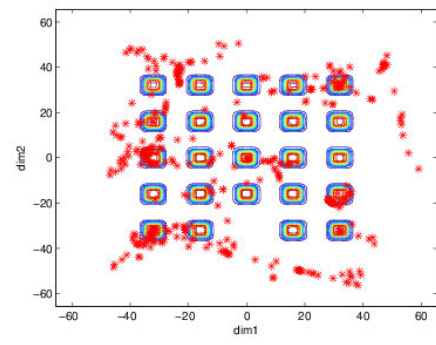
(a) a
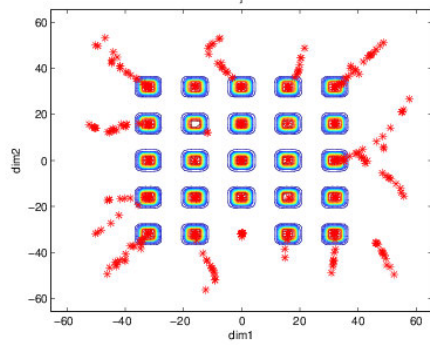
(b) b
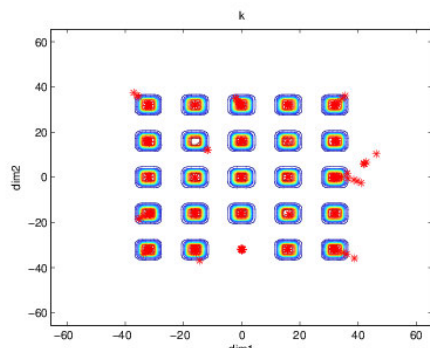
(c) c

(d) d

FIGURE 5. Glowworms' positions distribution for GSOM algorithm.

(a) a

(b) b

(c) c

(d) d

FIGURE 6. Glowworms' positions distribution for GSO algorithm.
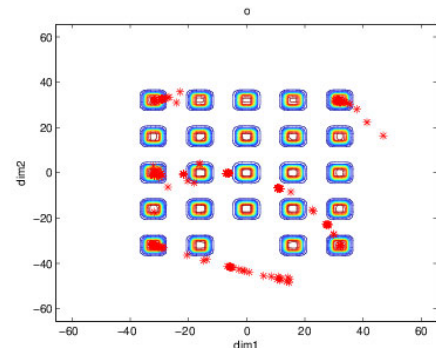
and LWGSODE (linearly weight glowworm swarm optimization differential evolution) algorithm, please refer to literature [38].
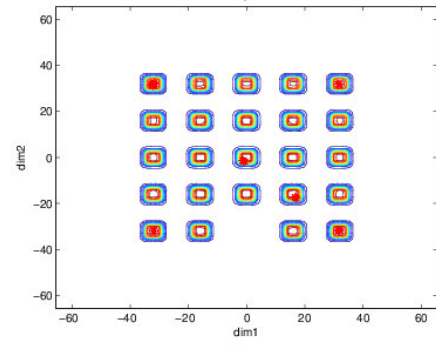
In the study, each function is in 20 dimensions and each function's fitness is its own value. Furthermore, all the functions' optimization experiments are conducted under the

TABLE 2. High-dimensional benchmark functions.

Benchmark functions	Domain	f_{min}
$f1 = \sum_{i=1}^{n} |x_i| + \prod_{i=1}^{n} |x_i|$	$[-10,10]^n$	0
$f2 = \sum_{i=1}^{n} (\sum_{j=1}^{i} x_j)^2$	$[-10,10]^n$	0
$f3 = \sum_{i=1}^{n} x_i^2$	$[-100,100]^n$	0
$f4 = \sum_{i=1}^{n} ix_i^4$	$[-10,10]^n$	0
$f5 = \sum_{i=1}^{n} (0.2x_i^2 + 0.1x_i^2 sin2x_i)$	$[-10,10]^n$	0
$f6 = \sum_{i=1}^{n} (x_i^2 - 10cos(2\pi x_i + 10)$	$[-5.12,5.12]^n$	0
$f7 = \frac{1}{4000} \sum_{i=1}^{n} x_i^2 - \prod_{i=1}^{n} (\frac{x_i}{\sqrt{i}}) + 1$	$[-32,32]^n$	0
$f8 = -20exp(-0.2\sqrt{\frac{1}{n}\sum_{i=1}^{n} x_i^2})$		
$-exp(\frac{1}{n}\sum_{i=1}^{n} cos(2\pi x_i)) + 20 + e$	$[-32,32]^n$	0
$f9 = \sum_{i=1}^{n-1} (100(x_{i+1} - x_i^2)^2 + (x_i - 1)^2)$	$[-30,30]^n$	0
$f10 = \sum_{i=1}^{n} x_i^2 + (\sum_{i=1}^{n} 0.5ix_i)^2$		
$+(\sum_{i=1}^{n} 0.5ix_i)^4$	$[-5,10]^n$	0

same condition, e.g. they all are conducted with the same MATLAB 2009 software and a windows 7 system.

Additionally, each experiment's swarm size is 40 and maximum iteration is set to be 1000. For GSO algorithm, the position update of each glowworm is based on Eq.(4) while for LWGSO, LWGSODE and GSOMLDW algorithms ω is adjusted according to Eq.(8). Especially, for GSOMLDW algorithm s1 is set to be 0.001 and s2 is set to be 0.0001.

Statistical results of 30 independent experiments are presented in table 3 and table 4.

In the experiment, each function itself is its own objective function. Our aim is to locate the point which makes the function value the smallest. Thus, a smaller optimization result means a better solution, and vice versa. Best solution, worst solution, mean solution, average standard deviation as well as consumed time over 30 runs for each algorithm have been given in the table 3 and table 4. From the numerical optimization results, it can be easily observed that GSOMLDW algorithm greatly outperforms GSO, LWGSO and LWGSODE algorithms with better optimization results. Meanwhile, standard deviations indicate the improved GSOMLDW algorithm has stronger robustness with lower or comparative standard deviations than GSO, LWGSO and LWGSODE algorithms.

Besides, each function's mobility of average fitness evaluation has been shown in Fig.7-Fig.9. As table 3 and table 4 illustrate, from the figures it can be obviously seen that experimental results are significantly different in aspects of average convergence speed and average convergence precision among the four algorithms.

As a short conclusion, although GSOMLDW needs a litter more time than GSO and LWGSO algorithm, it is faster than LWGSODE algorithm. Furthermore, it has faster convergence speed, higher convergence accuracy and stronger robustness when compared with other algorithms. The main reason exists in that the glowworm swarm diversity is preserved through mutation operation and moving step is adaptive based on dynamic inertia weight.

2) GSOMLDW ALGORITHM FOR SERVO SYSTEM IDENTIFICATION

In order to improve target tracking accuracy, the proposed GSOMLDW algorithm is firstly used to identify servo

TABLE 3. The performance comparison of GSO, LWGSO, LWGSODE and GSOMLDW algorithms for ten benchmark functions. In the table "Best", "Worst", and "Mean" indicate the best value, the worst value, and the mean value over 30 independent experimental runs.

Function	Algorithm	Best	Worst	Mean
$f1$	GSO	16.8047	30.3235	21.7270
	LWGSO	$3.7773e^{-4}$	0.0063	0.0063
	LWGSODE	0.0652	0.1142	0.0881
	GSOMLDW	$6.1654e^{-4}$	0.0061	0.0025
$f2$	GSO	52.4661	$5.1185e^{+2}$	$2.4502e^{+2}$
	LWGSO	$8.0189e^{-9}$	$7.5435e^{-6}$	$2.5553e^{-6}$
	LWGSODE	$2.0095e^{-7}$	$3.3449e^{-6}$	$1.1670e^{-6}$
	GSOMLDW	$1.6149e^{-10}$	$7.2810e^{-9}$	$1.7371e^{-9}$
$f3$	GSO	$2.8408e^{+4}$	$4.5355e^{+4}$	$3.7948e^{+4}$
	LWGSO	$1.1782e^{-8}$	$1.1084e^{-6}$	$2.3572e^{-7}$
	LWGSODE	$3.2648e^{-7}$	$3.8371e^{-7}$	$3.2911e^{-7}$
	GSOMLDW	$9.5521e^{-11}$	$4.8338e^{-8}$	$6.5911e^{-9}$
$f4$	GSO	$2.2894e^{+3}$	$7.8806e^{+3}$	$3.8834e^{+3}$
	LWGSO	$5.0940e^{-17}$	$4.0434e^{-12}$	$5.6885e^{-13}$
	LWGSODE	$1.2013e^{-13}$	$2.5246e^{-13}$	$1.6944e^{-13}$
	GSOMLDW	$3.4959e^{-22}$	$5.6575e^{-16}$	$8.2433e^{-17}$
$f5$	GSO	6.7190	13.2026	10.3631
	LWGSO	$1.6879e^{-9}$	$2.0338e^{-7}$	$5.4320e^{-8}$
	LWGSODE	$9.1827e^{-9}$	$1.0396e^{-8}$	$9.3021e^{-9}$
	GSOMLDW	$3.0575e^{-11}$	$5.1515e^{-9}$	$9.0906e^{-10}$
$f6$	GSO	74.8502	$1.3457e^{+2}$	$1.1135e^{+2}$
	LWGSO	$5.0188e^{-6}$	$1.9246e^{-4}$	$6.5769e^{-5}$
	LWGSODE	$9.1083e^{-6}$	$9.5299e^{-6}$	$9.1485e^{-6}$
	GSOMLDW	$2.4800e^{-8}$	$3.3953e^{-6}$	$9.1064e^{-7}$
$f7$	GSO	1.5798	1.8918	1.7252
	LWGSO	$3.6820e^{-10}$	$1.1362e^{-7}$	$1.9384e^{-8}$
	LWGSODE	$2.2484e^{-9}$	$5.8527e^{-9}$	$2.7903e^{-9}$
	GSOMLDW	$1.1047e^{-12}$	$2.0685e^{-9}$	$3.1749e^{-10}$
$f8$	GSO	19.1956	20.0339	19.7518
	LWGSO	$7.1396e^{-5}$	0.0014	$4.6000e^{-4}$
	LWGSODE	$1.9177e^{-4}$	$2.3618e^{-4}$	$1.9450e^{-4}$
	GSOMLDW	$2.2336e^{-5}$	$3.0809e^{-4}$	$9.2370e^{-5}$
$f9$	GSO	$4.1057e^{+7}$	$8.9373e^{+7}$	$6.5895e^{+7}$
	LWGSO	18.8279	18.9924	18.9367
	LWGSODE	18.9936	20.0577	19.1615
	GSOMLDW	18.8231	18.9691	18.9038
$f10$	GSO	$1.4780e^{+2}$	$1.8949e^{+7}$	$3.3834e^{+6}$
	LWGSO	$9.5843e^{-9}$	$1.2491e^{-6}$	$3.8646e^{-7}$
	LWGSODE	$5.6898e^{-8}$	$1.0640e^{-7}$	$7.2624e^{-8}$
	GSOMLDW	$1.9030e^{-10}$	$2.6724e^{-8}$	$4.5477e^{-9}$

system. In the part the GSOMLDW algorithm is used to identify a SISO system and a MISO system. In essential, identification is to search for the best non-linear combination of neural network's parameters so that the objective function value can reach a minimum. Consequently, the identification problem is actually a uni-modal optimization problem.

In detail, using neural networks to identify a nonlinear system is to approximate the system with the strong nonlinear mapping ability of the neural network. A neural network's feed-forward or regression structure, the neuron numbers in its input layer, hidden layer or output layer, its activation function types in the hidden layer as well as values of weights and biases of the neural network determine its nonlinear characteristics together. Essentially, this is a combinatorial optimization problem with constraints. Fortunately, the swarm intelligent algorithms can be used to solve the problem. Specifically, each glowworm individual's position is considered as a potential solution in the multidimensional solution

TABLE 4. The performance comparison of GSO, LWGSO, LWGSODE and GSOMLDW algorithms for ten benchmark functions. In the table "*Std .dev.*" indicates the standard deviation value over 30 independent experimental runs. "*times(s)*" denotes time cost by the corresponding function and algorithm.

Function	Algorithm	Std.dev.	times(s)
$f1$	GSO	3.3843	123.1831
	LWGSO	0.0013	90.7048
	LWGSODE	0.0137	156.7955
	GSOMLDW	0.0014	133.1388
$f2$	GSO	$1.5277e^{+2}$	115.3498
	LWGSO	$2.1340e^{-6}$	97.7723
	LWGSODE	$8.3764e^{-7}$	159.3936
	GSOMLDW	$1.5525e^{-9}$	150.4111
$f3$	GSO	$4.6253e^{+3}$	113.2514
	LWGSO	$2.4605e^{-7}$	86.1787
	LWGSODE	$1.0452e^{-8}$	149.9512
	GSOMLDW	$9.6060e^{-9}$	126.6921
$f4$	GSO	$1.3512e^{+3}$	118.9331
	LWGSO	$8.5297e^{-13}$	93.9795
	LWGSODE	$2.7308e^{-14}$	155.1737
	GSOMLDW	$1.2537e^{-16}$	132.8150
$f5$	GSO	2.0123	115.6748
	LWGSO	$4.3210e^{-8}$	87.8724
	LWGSODE	$2.8894e^{-10}$	148.8869
	GSOMLDW	$1.1410e^{-9}$	128.7680
$f6$	GSO	13.1923	108.7731
	LWGSO	$5.1485e^{-5}$	86.2940
	LWGSODE	$1.0719e^{-7}$	149.0257
	GSOMLDW	$8.9319e^{-7}$	130.0784
$f7$	GSO	0.0791	116.2189
	LWGSO	$2.1758e^{-8}$	90.5386
	LWGSODE	$6.3033e^{-10}$	151.1552
	GSOMLDW	$4.5068e^{-10}$	131.6051
$f8$	GSO	0.1784	115.3765
	LWGSO	$3.5480e^{-4}$	87.4257
	LWGSODE	$9.5884e^{-6}$	151.0561
	GSOMLDW	$6.1039e^{-5}$	129.4013
$f9$	GSO	$1.1177e^{+7}$	115.5837
	LWGSO	0.0316	88.3927
	LWGSODE	0.2463	147.5247
	GSOMLDW	0.0318	133.7174
$f10$	GSO	$6.1247e^{+6}$	115.3266
	LWGSO	$3.5532e^{-7}$	90.0290
	LWGSODE	$1.2048e^{-8}$	151.5287
	GSOMLDW	$5.8863e^{-9}$	129.2573

space. Here, each individual represents a combination of neural network's weights and thresholds. Through establishing the objective function, after several iterations glowworms gather at the optimal solution finally. Thus, the optimal combination of neural network parameters is achieved. Under this situation the specified neural network with the optimized parameters can approximate the identified system with the smallest mean square error.

Specifically, objective function in this paper is sum of mean square error, and variables are weights and thresholds of neural network. It is supposed that there is a three-layer feed-forward neural network with M inputs, N hidden layers, and K output units. The number of variables that need to be identified is $(M + 1)N + (N + 1)K$.

The fitness function is depicted as follows:

$$g = \frac{1}{Q}\Sigma_{i=1}^{Q}\Sigma_{q=1}^{K}(1/2)(P_i - P_i')^2 \qquad (14)$$
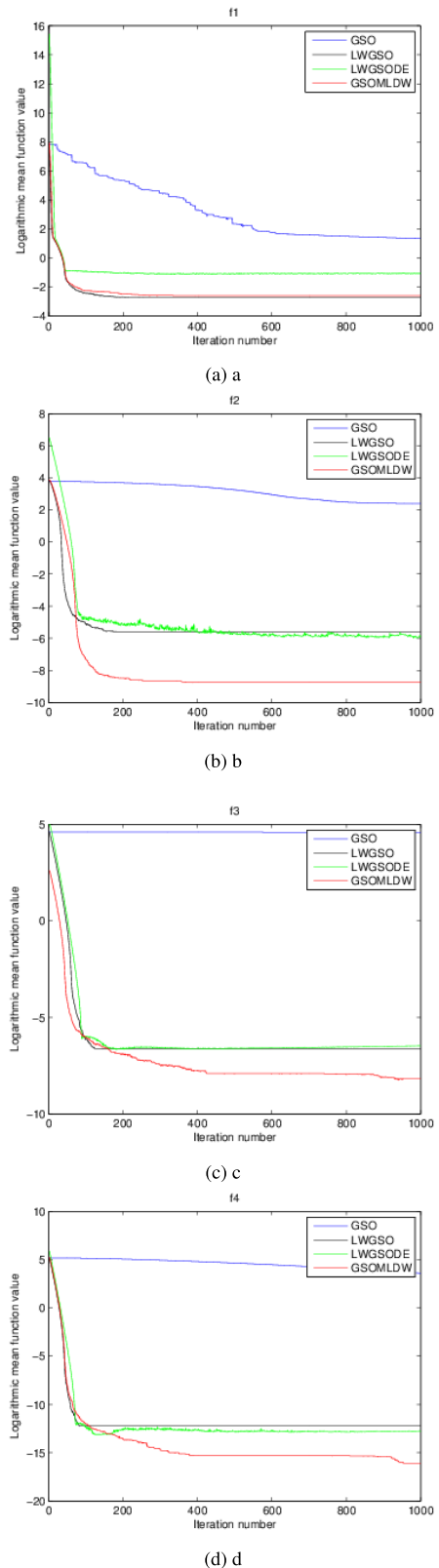

(a) a

(b) b

(c) c

(d) d

FIGURE 7. Average mobility of fitness comparison for $f1 - f4$.

where Q is the number of samples, P_i is the target output and P_i' is the output inferred from neural network.

In the glowworms' population, location of each glowworm individual can be expressed using those variables.
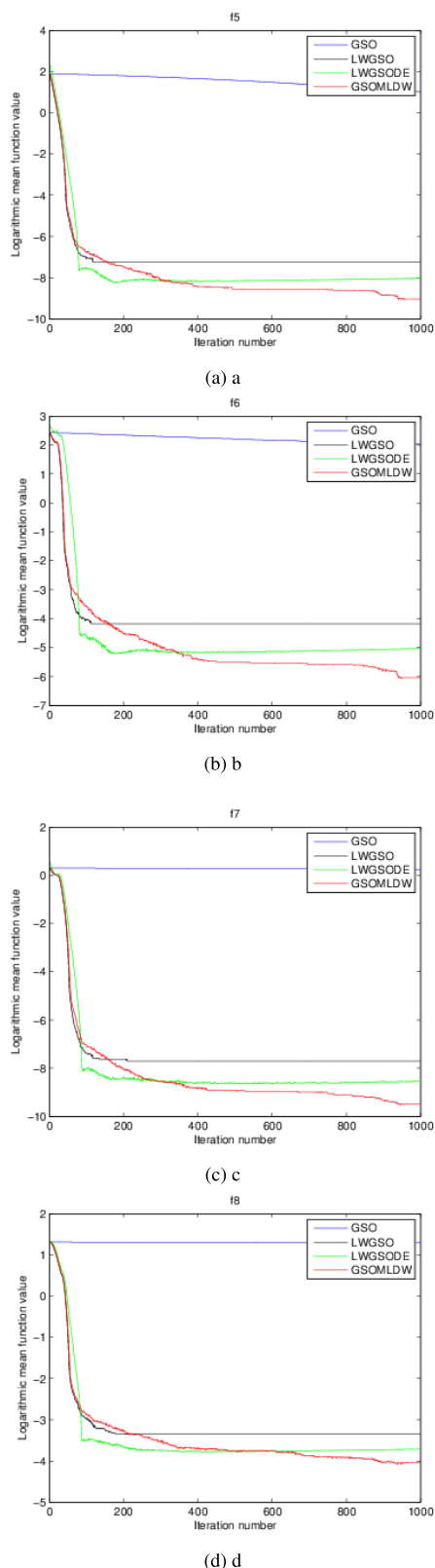
(a) a

(b) b

(c) c

(d) d

FIGURE 8. Average mobility of fitness comparison for $f5 - f8$.

Through the whole searching process, glowworm individuals will eventually gather at the position where the fitness function reaches the extreme value. Finally the network can be obtained, which can approximate the identified model.
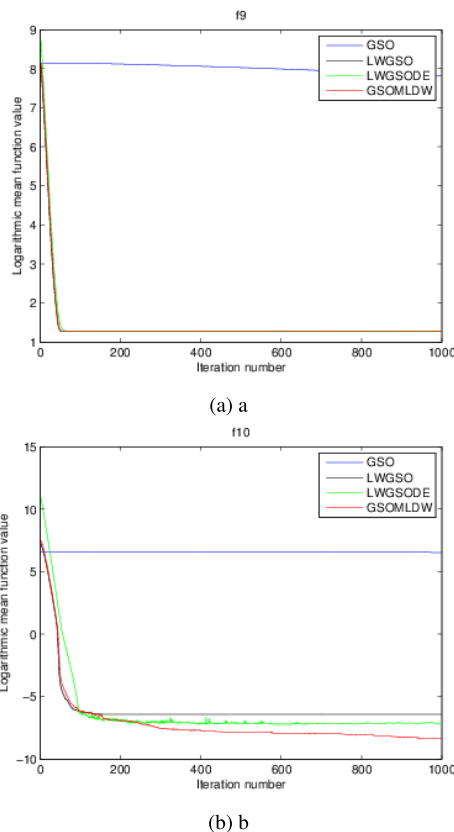

(a) a

(b) b

FIGURE 9. Average mobility of fitness comparison for $f9$ and $f10$.

In the study, except for GSOMLDW algorithm, PSO, GSO and LWGSO [38] algorithms have also been utilized to identify systems.

Here, SISO system is a nonlinear function which is depicted as below:

$$y = sin(2x)e^{-2x} \qquad (15)$$

In order to identify the system, the population size is set to be 30. The maximum iteration is set to be 2000. Moving step s is set to be 0.01. For the GSOMLDW algorithm, except for the above mentioned parameters, moving step $s1$ is set to be 0.02 and moving step $s2$ is set to be 0.005. The derived statistical results over 10 times of independent experiments for the four algorithms have been shown in table 5.

TABLE 5. Training performance comparison for SISO system identification. In the table, "*Best*", "*Worst*", "*Mean*" and "*Std.dev.*" denote the best value, the worst value, the mean value and the standard deviation among multiple runs, respectively.

	PSO	GSO	LWGSO	GSOMLDW
Best	$4.62e^{-3}$	1.063	0.0010	$8.40e^{-5}$
Worst	0.02	63.50	0.0036	0.0016
Mean	0.0015	28.65	0.0022	$5.33e^{-4}$
Std.dev.	0.05	19.02	$4.83e^{-4}$	$3.10e^{-4}$
Time	355.56	45.96	47.53	79.46

From table 5, it can be easily concluded that GSOMLDW is undoubtedly the best one compared with the other four swarm

intelligence algorithms. Specifically, it can be clearly seen from table 4 that the optimal solution obtained during 10 runs is $8.4e^{-5}$. It is the minimum solution obtained among PSO, GSO, LWGSO, and GSOMLDW algorithms. Furthermore, the GSOMLDW algorithm is also one of the best performing algorithms in terms of other items of statistical results, such as worst solution, mean value, and standard deviation. Unfortunately, the original GSO algorithm is worse than other algorithms in terms of worst solution, optimal solution, average value, and standard deviation items. In addition, the time of each simulation run has been recorded for 10 independent simulations. The average running time of each algorithm is obtained. As shown in the last row of table 5, it can be clearly seen from the results that the calculation time of the GSOMLDW algorithm, the GSO algorithm, and the LWGSO algorithm is equivalent.

Fig.10 shows fluctuation of the fitness function when the SISO system is identified using the GSOMLDW algorithm. Here, the squares sum inverse of the difference between the neural network output and the actual value of the function is selected as the fitness function during the training process. As can be seen from this figure, the function drops rapidly as the number of iterations increases, and it is soon close to zero. This phenomenon fully demonstrates that the search efficiency of the algorithm is high.

In Fig.10, figure b provides comparison of the real model and the best approximation result. The blue line is relationship of the independent variable x and the dependent variable y for the actual model. The red line is relationship of the independent variable x and the output of a three-layer neural network optimized by GSOMLDW algorithm. It can be easily seen from the figure that the identified model obtained by the proposed algorithm can approximate the actual system.

The approximation error is also shown in Fig.10. Figure c is the error between actual outputs and outputs of identified model. The figure illustrates that the approximation error is up to 0.05 and the minimum approximation error is below 0.01. Therefore, effectiveness of the proposed identification method is fully explained.

Different from identification of a SISO system, identification of a MISO system is much more complex. The expression of the MISO system is written as below:

$$x(t+1) = \frac{x(t)x(t-1)[x(t)+2.5]}{1+x^2(t)+x^2(t-1)+\sin(\frac{4\pi t}{25})} \quad (16)$$

In the identification experiment for MISO system, fifty pairs of data from t = 0 to t = 50 are used as training samples. Glowworm swarm size and maximum iteration is set 30 and 200, respectively. Moving step *s* is set to be 0.01. For the GSOMLDW algorithm, except for the above mentioned parameters, moving step *s*1 is set to be 0.01 and moving step *s*2 is set to be 0.008. In the section, when the neural network's structure is the same as $1 \times 10 \times 1$, optimization results with different intelligence optimization algorithms are compared in table 6.
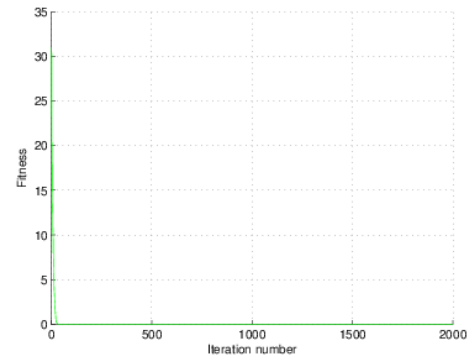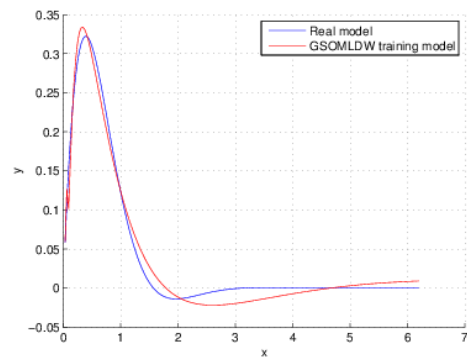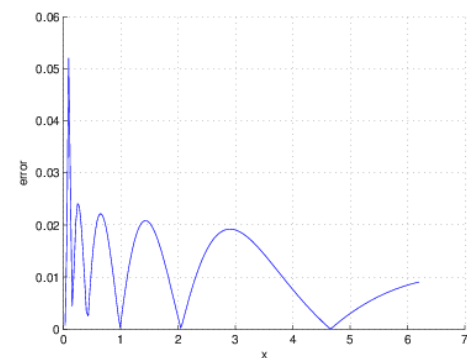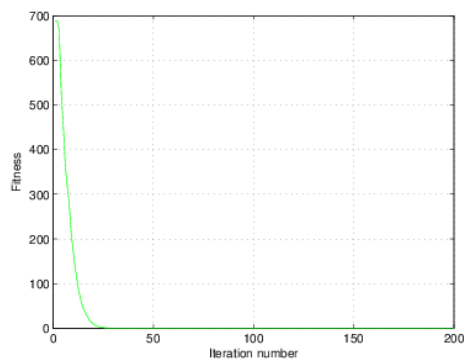

FIGURE 10. Experimental results for SISO system identification.

TABLE 6. Training performance comparison for MISO system identification. In the table, *"Best"*, *"Worst"*, *"Mean"* and *"Std .dev."* denote the best value, the worst value, the mean value and the standard deviation among multiple runs, respectively.

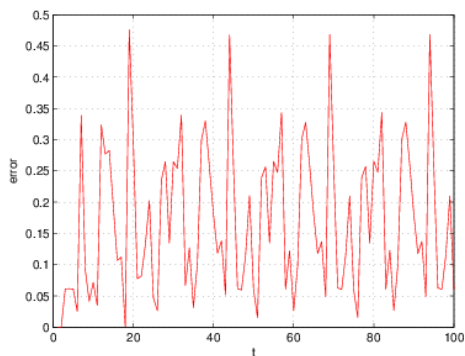|	PSO	GSO	LWGSO	GSOMLDW
Best	0.1399	94.91	0.1438	0.0174
Worst	5.387	657.98	0.3879	0.2450
Mean	0.6743	403.44	0.2622	0.1232
Std.dev.	1.035	148.92	0.0569	0.0557
Time	131.83	10.8	11.17	13.8

It can be clearly seen from table 6 that during 10 independent runs, the GSOMLDW algorithm obtains the optimal solution of 0.0174, the worst value of 0.2450, and the average
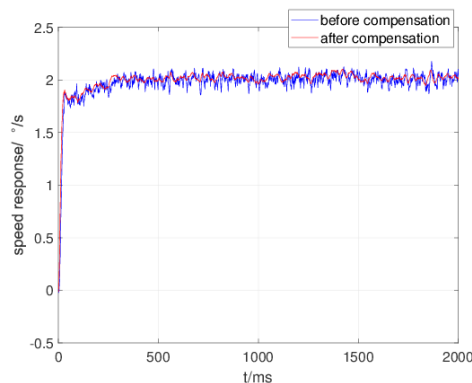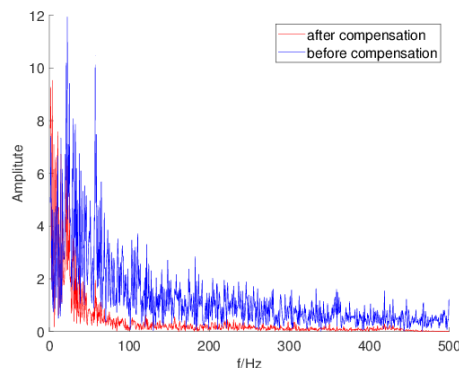
(a) a
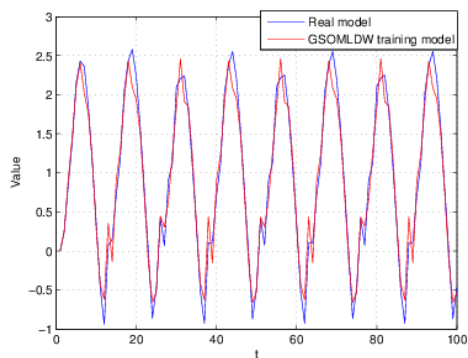
(b) b

(c) c

FIGURE 11. Experimental results for MISO system identification.

(a) a

(b) b

(c) c

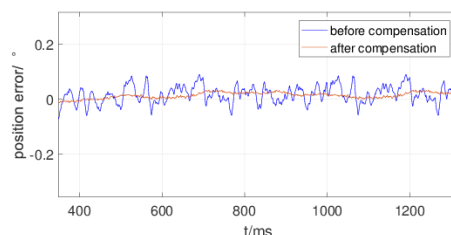**FIGURE 12. Experimental results for target tracking.**

value of 0.1232. In these three aspects, GSOMLDW performs better than the other three methods. In terms of standard deviation, the results of the GSOMLDW algorithm and the LWGSO algorithm are comparable, and both of them are close to 0.05. However, the GSO algorithm performs the worst, and the result is far worse than the other methods in all aspects. The LWGSO algorithm is relatively better than the PSO algorithm, but is slightly worse than GSOMLDW algorithm. In addition, we recorded the time of each simulation run for 10 independent simulation times and obtained the average running time of each algorithm, as shown in the last row of table 6. It can be clearly seen from the results that

calculation time of the GSOMLDW algorithm, the GSO algorithm, and the LWGSO algorithm is equivalent, and the PSO algorithm runs the longest time. Therefore, table 6 illustrates GSOMLDW algorithm is obviously the best one among the four swarm intelligence algorithms.

Fig.11 provides mobility of fitness when using the GSOMLDW algorithm to identify the MISO system. Here again, the inverse square sum of difference between the neural network output and the actual value is selected as the training fitness. As can be seen from the figure, fitness value drops rapidly from 700. After about 25 iterations, fitness value is close to zero. This phenomenon fully demonstrates that search efficiency of the algorithm is high.

In Fig.11, figure b shows the real output and the best identification result by using GSOMLDW algorithm. As can be seen from this figure, the red line and the blue line are

basically coincident. It illustrates that the proposed algorithm is effective for not only SISO system but also MISO system. It fully demonstrates applicability of the proposed algorithm.

The approximation error is shown in Fig.11. In Fig.11 figure c is approximation error between the actual outpt and the output of the neural network model. It can be seen from the figure that approximation error is up to 0.5 and at most of time the error is concentrated around 0.3. The result fully explains the effectiveness of the identification algorithm proposed in this paper.

3) GSOMLDW ALGORITHM FOR TRACKING ACCURACY IMPROVEMENT

The closed-loop velocity response of azimuth axis before and after compensation of gyro error and the corresponding spectrum curves have been shown in figure 12. It can be clearly seen from the figure that the steady-state error of the speed step response after compensation is satisfactory. From the spectrum analysis curve in figure b, it is easier to see that the low-frequency energy of the gyro signal after compensation is significantly reduced, indicating that the low-frequency error compensation method is significantly effective. Additionally, position error fluctuation comparison before and after compensation has been shown in figure c. It can be easily concluded that without compensation position error range is within $1500\ urad$, while the position fluctuation is almost to zero after compensation.

VI. CONCLUSION

In order to improve target detection rate and tracking accuracy, in regard to GSO's shortcomings of low peak detection rate and low optimization accuracy, there are two methods proposed in the paper to improve GSO's performance. Firstly, as to GSO's deficiency of lack of search history memory, a GSOM algorithm is proposed. When an individual gets into traps and there are no better neighborhoods, the proposed GSOM algorithm will produce a new individual according to the best solution found during search history. Experimental results of four multi-modal benchmark functions have illustrated that the proposed GSOM algorithm can make fully use of all glowworms' search histories and locate more optima than GSO algorithm. Then, based on the proposed GSOM algorithm, a complex multi-modal function is optimized. The optimization results show that GSOM algorithm can obtain more optimal hyper-parameter combinations, which is beneficial for detecting multi-target. Secondly, for the problem that fixed movement step causes shock phenomenon near peaks, which may reduce algorithm's convergence rate and weaken accuracy of the final optimization result, glowworms' positions are updated based on dynamic inertia weight. Meanwhile, the proposed GSOMLDW algorithm's convergency proof has been provided in the paper. Experiments on optimization of ten classic uni-modal benchmark functions have been conducted. After that, aiming at improving target servo tracking accuracy a multi-layer feed-forward network is constructed to identify servo systems. Comparison results with

other intelligent algorithms in terms of identification accuracy, fastness, robustness and computational complexity have fully confirmed the proposed GSOMLDW algorithm's superiority. Importantly, the proposed GSOMLDW algorithm is used to compensate for the drift error. Final results show that the position error fluctuation after compensation is almost zero while before compensation it reaches $1500\ urad$. Consequently, the proposed methods can effectively improve target detection rate and tracking precision. In future work we will apply both of the improved algorithms to solve many other complex mechanical engineering problems.

REFERENCES

[1] T. Hayajneh, R. Doomun, G. Al-Mashaqbeh, and B. J. Mohd, "An energy-efficient and security aware route selection protocol for wireless sensor networks," *Secur. Commun. Netw.*, vol. 7, no. 11, pp. 2015–2038, Nov. 2014.

[2] S. Wang, X. Lu, Q. Wang, L. Wei, and R. Huang, "Hardware architecture design of multi-target detection and tracking system," in *Proc. Electr. Control Eng. Mater. Sci. Manuf.*, Apr. 2016, pp. 241–247.

[3] F. Lin, K.-Y. Lum, B. M. Chen, and T. H. Lee, "Development of a vision-based ground target detection and tracking system for a small unmanned helicopter," *Sci. China Ser. F, Inf. Sci.*, vol. 52, no. 11, pp. 2201–2215, Nov. 2009.

[4] J. Bergstra and Y. Bengio, "Random search for hyper-parameter optimization," *J. Mach. Learn. Res.*, vol. 13, pp. 281–305, Feb. 2012.

[5] H. Xiang, "Adaptive friction compensation based on LuGre model," *J. Mech. Eng.*, vol. 48, no. 17, p. 70, 2012.

[6] X. Wang and S. Wang, "High performance adaptive control of mechanical servo system with LuGre friction model: Identification and compensation," *J. Dyn. Syst., Meas., Control*, vol. 134, no. 1, Jan. 2012.

[7] Z.-Q. Mei, Y.-C. Xue, and R.-Q. Yang, "Nonlinear friction compensation in mechatronic servo systems," *Int. J. Adv. Manuf. Technol.*, vol. 30, nos. 7–8, pp. 693–699, Oct. 2006.

[8] Y. Sun, W. Xiong, Z. Yao, K. Moniz, and A. Zahir, "Analysis of network attack and defense strategies based on Pareto optimum," *Electronics*, vol. 7, no. 3, p. 36, 2018.

[9] L. Qing, W. Gang, Y. Zaiyue, and W. Qiuping, "Crowding clustering genetic algorithm for multimodal function optimization," *Appl. Soft Comput.*, vol. 8, no. 1, pp. 88–95, Jan. 2008.

[10] S.-H. Xu, J.-P. Liu, F.-H. Zhang, L. Wang, and L.-J. Sun, "A combination of genetic algorithm and particle swarm optimization for vehicle routing problem with time windows," *Sensors*, vol. 15, no. 9, pp. 21033–21053, 2015.

[11] T. Yifei, Z. Meng, L. Jingwei, L. Dongbo, and W. Yulin, "Research on intelligent welding robot path optimization based on GA and PSO algorithms," *IEEE Access*, vol. 6, pp. 65397–65404, 2018.

[12] X. S. Yang, "Firefly algorithm, Levy flights and global optimization," in *Research and Development in Intelligent Systems*, M. Bramer, R. Ellis, M. Petridis, Eds. London, U.K.: Springer, 2010, pp. 209–218.

[13] R. M. Luque-Baena, J. M. Ortiz-de-Lazcano-Lobato, E. López-Rubio, E. Domínguez, and E. J. Palomo, "A competitive neural network for multiple object tracking in video sequence analysis," *Neural Process. Lett.*, vol. 37, no. 1, pp. 47–67, Feb. 2013.

[14] X. S. Yang, "Firefly algorithms for multimodal optimization," in *Stochastic Algorithms: Foundation Application*. Berlin, Germany: Springer, 2009, pp. 169–178.

[15] M. G. Li, M. Li, G. P. Han, N. Liu, Q. M. Zhang, and Y. O. Wang, "Optimization analysis of the energy management strategy of the new energy hybrid 100% low-floor tramcar using a genetic algorithm," *Appl. Sci.*, vol. 8, p. 1144, Jun. 2018.

[16] S. Kirkpatrick, "Optimization by simulated annealing: Quantitative studies," *J. Stat. Phys.*, vol. 34, nos. 5–6, pp. 975–986, Mar. 1984.

[17] Y. Zhou, X. Li, and L. Gao, "A differential evolution algorithm with inter-sect mutation operator," *Appl. Soft Comput.*, vol. 13, no. 1, pp. 390–401, Jan. 2013.

[18] S. Mirjalili, S. Z. Mohd Hashim, and H. Moradian Sardroudi, "Training feedforward neural networks using hybrid particle swarm optimization and gravitational search algorithm," *Appl. Math. Comput.*, vol. 218, no. 22, pp. 11125–11137, Jul. 2012.

[19] X. Wu, F. Deng, and Z. Chen, "RFID 3D-LANDMARC localization algorithm based on quantum particle swarm optimization," *Electronics*, vol. 7, no. 2, p. 19, 2018.

[20] T. H. Tan, B. A. Chen, and Y. F. Huang, "Performance of resource allocation in device-to-device communication systems based on evolutionally optimization algorithms," *Appl. Sci.*, vol. 8, no. 8, p. 1271, 2018.

[21] S. Qin, Y. Zhang, Y.-L. Zhou, and J. Kang, "Dynamic model updating for bridge structures using the kriging model and PSO algorithm ensemble with higher vibration modes," *Sensors*, vol. 18, no. 6, p. 1879, 2018.

[22] X. Li, J. Guo, and J. Hu, "An improved PSO algorithm and its application in GNSS ambiguity resolution," *Appl. Sci.*, vol. 8, no. 6, p. 990, 2018.

[23] W. Hu, L. Yan, K. Liu, and H. Wang, "A short-term traffic flow forecasting method based on the hybrid PSO-SVR," *Neural Process. Lett.*, vol. 43, no. 1, pp. 155–172, Feb. 2016.

[24] W. M. Gao, "Study on the firefly algorithm and applications," Lanzhou Univ., Lanzhou, China, Tech. Rep., 2013.

[25] S. J. Kang, "Research and improvement of Glowworm Swarm optimization algorithm," Guangdong Univ. Technol., Guangzhou, China, Tech. Rep., 2013.

[26] F. G. Liu and D. X. Zhong, "GSOS-ELM: An RFID-based indoor localization system using GSO method and semi-supervised online sequential ELM," *Sensors*, vol. 18, no. 7, p. 195, 2018.

[27] Y. Zhou, Q. Luo, and J. Liu, "Glowworm swarm optimization for dispatching system of public transit vehicles," *Neural Process. Lett.*, vol. 40, no. 1, pp. 25–33, Aug. 2014.

[28] K. N. Krishnanand and D. Ghose, "Glowworm swarm based optimization algorithm for multimodal functions with collective robotics applications," *Multiagent Grid Syst.*, vol. 2, no. 3, pp. 209–222, Sep. 2006.

[29] K. N. Krishnanand and D. Ghose, "A glowworm swarm optimization based multi-robot system for signal source localization," *Design and Control of Intelligent Robotic Systems*. Berlin, Germany: Springer-Verlag, 2009, pp. 49–68.

[30] J. Wang, Y. Q. Cao, J. Y. Cao, H. Ji, and X. F. Yu, "Virtual force and glowworm swarm optimization based node deployment strategy for WSNs," *Advances in Computer Science and Ubiquitous Computing*, pp. 456–462, 2016.

[31] M. Lu, H. Wang, J. Lin, A. Yi, Y. Gu, and D. Zhao, "A nonlinear Wiener system identification based on improved adaptive step-size glowworm swarm optimization algorithm for three-dimensional elliptical vibration cutting," *Int. J. Adv. Manuf. Technol.*, vol. 103, nos. 5–8, pp. 2865–2877, Aug. 2019.

[32] P. Pandey, A. Shukla, and R. Tiwari, "Three-dimensional path planning for unmanned aerial vehicles using glowworm swarm optimization algorithm," *Int. J. Syst. Assurance Eng. Manage.*, vol. 9, no. 4, pp. 836–852, Aug. 2018.

[33] Z. H. Hu, Y. G. Han, L. Cao, and Y. Bai, "A CWMN spectrum allocation based on multi-strategy fusion glowworm swarm optimization algorithm," *Wireless Internet*, vol. 22, pp. 109–120, 2017.

[34] R. Z. Chen, "Improved self-adaptive glowworm swarm optimization algorithm," *Appl. Mech. Mater.*, vols. 519–520, pp. 798–801, Feb. 2014.

[35] J. Xin, G. Chen, and Y. Hai, "A particle swarm optimizer with multi-stage linearly-decreasing inertia weight," in *Proc. Int. Joint Conf. Comput. Sci. Optim.*, Apr. 2009, pp. 505–508, doi: 10.1109/cso.2009.420.

[36] M. Xi, J. Sun, and W. Xu, "An improved quantum-behaved particle swarm optimization algorithm with weighted mean best position," *Appl. Math. Comput.*, vol. 205, no. 2, pp. 751–759, Nov. 2008.

[37] X. Li, "Niching without niching parameters: Particle swarm optimization using a ring topology," *IEEE Trans. Evol. Comput.*, vol. 14, no. 1, pp. 150–169, Feb. 2010.

[38] H. Cui, J. Feng, J. Guo, and T. Wang, "A novel single multiplicative neuron model trained by an improved glowworm swarm optimization algorithm for time series prediction," *Knowl.-Based Syst.*, vol. 88, pp. 195–209, Nov. 2015.

XINGKUI XU received the M.S. degree in information and communication engineering from Xidian University, Xi'an, China, in 2007. He is currently pursuing the Ph.D. degree in space optoelectronics science and technology with the Harbin Institute of Technology, Harbin, China.

He is also with the Harbin Institute of Technology. His main research interests include optimization algorithms, servo control, and target detection.
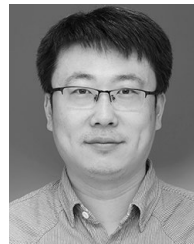
QINGYU HOU was born in China, in 1982. He received the master's and Ph.D. degrees in optical engineering from the Harbin Institute of Technology, Harbin, China, in 2006 and 2011, respectively.

He is currently an Associate Professor and a Ph.D. Supervisor of optical engineering with the Harbin Institute of Technology.

CHUNFENG WU received the Ph.D. degree from the Harbin Institute of Technology, Harbin, China.

He is currently a Researcher with China Space Sanjiang Group Corporation Ltd. He is also a Ph.D. Supervisor with the Space Optical Engineering Research Center, Harbin Institute of Technology.

ZHIGANG FAN received the master's degree in electrical engineering and the Ph.D. degree from the Harbin Institute of Technology, Harbin, China, in 1992 and 2004, respectively.

Since 1992, he has been a Teacher with the Harbin Institute of Technology. He is currently the Deputy Director and a Ph.D. Supervisor with the Space Optical Engineering Research Center, Harbin Institute of Technology.

● ● ●